Computational catalysis

A computational study of phosphine ligand effects in Suzuki–Miyaura coupling☆

Jesús Jover [a], Natalie Fey [a], Mark Purdie [b], Guy C. Lloyd-Jones [a], Jeremy N. Harvey [a],*

[a] School of Chemistry, University of Bristol, Cantock's Close, Bristol BS8 1TS, UK
[b] AstraZeneca, Bakewell Road Loughborough, LE11 5RH, UK

ARTICLE INFO

ABSTRACT

DFT calculations have been used to explore the full catalytic cycle of the Suzuki–Miyaura coupling between PhBr and $PhB(OH)_3^-$ with four different palladium monophosphine catalysts derived from $Pd(PMe_3)_2$, $Pd(P(CF_3)_3)_2$, $Pd(PPh_3)_2$ and $Pd(P^tBu_3)_2$. All the steps of the reaction have been studied and the differences between the ligands have been analyzed; special attention has been devoted to the ligand dissociation and catalyst regeneration processes, as well as the typical cross-coupling steps of oxidative addition, transmetallation and reductive elimination. Multiple linear regressions of the computationally derived energy barriers have been carried out in order to quantify the ligand effects of the different phosphines on the key steps of the reaction. These ligand effects, relevant to the catalytic activity, are described in terms of the phosphine donor/acceptor and steric features. The regression models show that oxidative addition is mainly governed by electronic effects whereas the transmetallation and the reductive elimination processes are controlled by a mixture of both ligand effects. For transmetallation, electron-withdrawing ligands lower the energy barrier.

© 2010 Elsevier B.V. All rights reserved.

1. Introduction

The Suzuki–Miyaura coupling is one of the most widely used methods for the formation of carbon–carbon bonds. In this reaction an organoboron compound (normally an organoboronic acid) is coupled with an organic halide or triflate in the presence of a palladium catalyst and a base [1] (Eq. (1)). The high tolerance of the reaction conditions towards functional groups, as well as the low toxicity and ready availability of boronic acids have made these latter one of the favourite reagents in cross-coupling reactions [2–11].

$$R - B(OH)_2 + R' - X \xrightarrow[\text{base}]{[Pd]} R - R' + X - B(OH)_2 \quad (1)$$
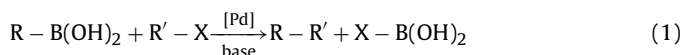
The main steps in the generally accepted catalytic cycle for the Suzuki–Miyaura coupling are shown in Scheme 1. Many of these steps are identical to or analogous to processes that occur in other palladium-catalyzed cross-coupling reactions. The potential applications of this reaction in organic synthesis have been studied from both experimental [2,7,12–16] and computational [17–21] points of view.

Among all the existing catalysts for this reaction, the most effective are the palladium/ligand systems. Recently, the introduction of sterically bulky, electron-rich ligands [7,22–28] has enabled many

of the previous experimental limitations of the Suzuki–Miyaura coupling reaction to be overcome. For example, it is now possible to use less reactive aryl chloride electrophiles [3], to work with sterically hindered systems [29], to incorporate alkyl chlorides and alkyl boron partners [30], and to use lower reaction temperatures and catalyst loadings [24]. The preferred ligands for this cross-coupling reaction are usually phosphines although carbenes have also proven successful [31–36].

One of the most controversial points when using palladium/phosphine systems as catalyst is the nature of the active catalytic species. Frequently, two equivalents of phosphine are either present in the catalyst precursor or added in the mixture, and it is at first sight reasonable to assume that they remain on the metal throughout the whole reaction. However, bulky electron-rich phosphines tend to increase the reaction performance and it has been proposed that monophosphine species can act as catalysts as well [12,25,29,37–43].

Computational studies dealing with individual steps related to this reaction such as oxidative addition [41,42,44–50], transmetallation [4,18,51–55] or reductive elimination [56–59] have been published as well as some that analyze the full catalytic cycle of the Suzuki–Miyaura coupling [19,40,60]. In most of these publications, model systems are used to describe the phosphines: PH_3 or PMe_3; or the reactants: vinyl instead of aryl. Hence computational studies of this reaction with real catalysts and substrates are relatively scarce in the literature. In this work, new density functional theory (DFT) calculations on the full catalytic cycle of the Suzuki–Miyaura coupling between PhBr and $PhB(OH)_3^-$ are reported. The
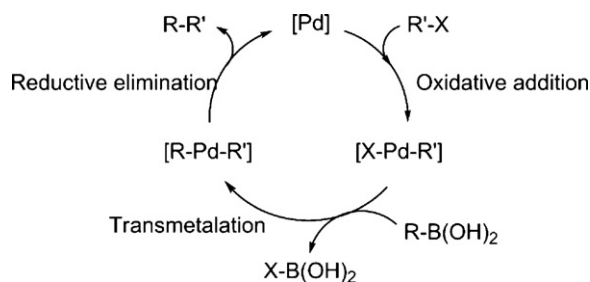
Scheme 1. General catalytic cycle for the Suzuki–Miyaura coupling.

reaction is studied using different palladium monophosphine catalysts derived from PMe$_3$, P(CF$_3$)$_3$, PPh$_3$ and P^{t}Bu$_3$. These four phosphines cover a wide range of electronic and steric features of this ligand family. Some additional calculations with the simpler, less realistic, PH$_3$ ligand were also carried out, and the results, not reported in detail here, are in very good agreement with previous B3LYP calculations on the same species [18].

Besides analyzing the common steps in cross-coupling reactions, namely oxidative addition, transmetallation and reductive elimination, special attention has been devoted to the less studied steps of the reaction such as the catalyst activation and regeneration. We have made one assumption concerning the degree of ligation of the metal centre. There is significant evidence [41–43] that for large, synthetically relevant, electron-rich phosphine ligands such as P^{t}Bu$_3$, most of the key intermediates in the catalytic cycle involve only a single phosphine ligand. Though this could in principle be different for other ligands, we have chosen to model all species in the catalytic cycle except the starting Pd(PR$_3$)$_2$ as involving a single phosphine ligand. A further reason to prefer a single ligand is that it has been found previously that oxidative addition to Pd(0) is much more facile when there is a single ligand bonded to palladium [61].

We use the well-established B3LYP functional throughout in our DFT calculations. Recent work suggests that this functional is not quantitatively accurate due among other deficiencies to the neglect of dispersion effects. This error can be particularly relevant when considering ligand dissociation from metal complexes [62–65], and further work might therefore be needed to obtain quantitative results. However, we expect that when comparing ligands, errors should broadly cancel.

Also, detailed statistical analysis has been used to get a better understanding of the ligand electronic and steric effects in the oxidative addition, transmetallation and reductive elimination steps [66,67]. In previous work, we [67,68] and others [69,70] have found that greater insight into ligand effects can be obtained by calculating relevant properties for multiple ligands and carrying out a statistical analysis of the results. Here, we use our existing Ligand Knowledge Base [68] of computed descriptors of phosphine ligands to construct multilinear regression models for the DFT energy barriers obtained for the key steps in the catalytic mechanism.

2. Computational details

All calculations were carried out using the Jaguar 6.0 package (Jaguar, Schrödinger, LLC, New York, NY, 2005) [71]. Geometry optimization in vacuum was carried out for all species at the B3LYP level of theory using the standard 6-31G(d) basis set for all atoms except Pd and Br. The Los Alamos ECP and associated LACV3P triple zeta basis set was used to describe the Pd and Br atoms. As noted above, the B3LYP functional does not describe non-bonding dispersion interactions very well [62–65,72], but it was nevertheless used here for consistency with previous studies [18,19] of some of the individual reaction steps. For all the studied species, geometry

optimization was carried out using standard geometry convergence criteria as well as ultrafine DFT and pseudospectral grids. Frequency calculations were carried out on most of the resulting refined structures in the case of reactions with the simplest phosphine (PMe$_3$), thereby providing values for the zero point energy (zpe) correction. The same zpe correction was used for the reactions of all phosphines.

The nature of the oxidative addition, transmetallation and reductive elimination transition states was additionally verified by computing vibrational frequencies for these TSs with all the phosphine ligands; a single imaginary frequency was obtained in all cases, corresponding to the expected reaction coordinate. For the substitution TSs Pd(PR$_3$)$_2$ + PhBr → Pd(PR$_3$)(PhBr) + PR$_3$ and Pd(PR$_3$)(PhPh) + PR$_3$ or PhBr → PhPh + Pd(PR$_3$)$_2$ or Pd(PR$_3$)(PhBr), frequency calculations were only performed for the case of PMe$_3$. Manual scans along the expected reaction coordinate in the region of the TS were used in the case of the other phosphines to confirm that these TSs did indeed correspond to the correct chemical transformation. In our discussion, we focus on calculated potential energies rather than free energies, partly due to the expense associated with carrying out frequency analysis for all species, and partly due to the uncertainties associated with calculations of free energies in solution [72]. We note that when comparing individual reaction steps with different ligands, entropic effects should broadly cancel out. Nevertheless, where relevant, some comments about expected entropic trends are included below.

To evaluate the solvent effect, single point calculations, using the Poisson–Boltzmann polarizable continuum model implemented in Jaguar [73,74], were performed on all the optimized gas phase geometries using the same level of theory and basis sets as above. Tetrahydrofuran (radius of solvent probe molecule = 2.52664 Å, outer dielectric constant = 7.52) was selected as solvent, as it is commonly used in Suzuki–Miyaura coupling experiments.

3. Results and discussion

3.1. Mechanism of PdPR$_3$-catalyzed Suzuki–Miyaura coupling

In this section, we describe the calculations used to explore the mechanism of all the steps hypothetically involved in the Suzuki–Miyaura coupling. We also discuss the similarities and differences between the structures and energies found for the four studied phosphine ligands. A detailed scheme of the catalytic cycle, including all the steps we have studied for the reaction between PhBr and PhB(OH)$_3^-$, is provided in Scheme 2. Scheme 3 shows the general potential energy surface for this catalytic cycle. The zero point corrected calculated energies for each species and for each ligand can be found in Table 1.

As mentioned in Section 2, single point energies have been computed for almost all species including a continuum model of THF solvent. The corresponding relative energies including the continuum free energy of solvation are shown in Table 2. The key difference between the results in Tables 1 and 2 occurs for the step in which the palladium-bound bromide undergoes exchange with the boronate PhB(OH)$_3^-$ derived from the reactant boronic acid. Bromide is a smaller ion than the boronate, and hence has a larger solvation free energy, so that this exchange step is predicted to be more favourable in continuum solvent than in vacuum, by ca. 15–20 kcal/mol. Also, oxidative addition to form (**4**) from (**3**) is found to be more exothermic in the presence of continuum solvent, e.g. ΔE is −15.3 kcal/mol with the P^{t}Bu$_3$ ligand in vacuo, and −24.1 kcal/mol with THF continuum. This stabilizing effect of the more polar Pd(II) oxidative addition product had been noted by others previously [75]. Other steps are significantly less affected, with barrier heights or reaction energies for individual steps typically
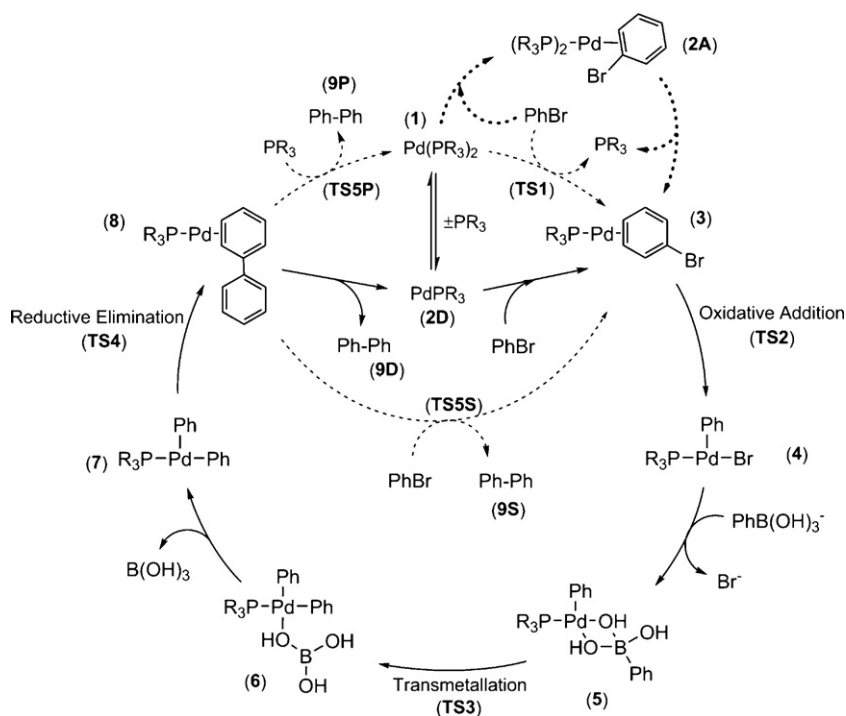
Scheme 2. Extended Suzuki–Miyaura catalytic cycle.

differing by less than 5 kcal/mol between the vacuum and continuum solvent calculations. Differences between barrier heights obtained using different ligands, a particular point of focus of this study, are not strongly affected by the presence of solvation.

Our discussion below uses vacuum energies almost exclusively. At first sight, the values obtained using continuum solvent might appear to be preferable, but there is relatively little difference for key energetics. We note also that there are likely to be discrepancies when comparing both the vacuum and continuum-derived energies with experiment. In particular, the 'real' reaction system involves counter-ions, and hence, in the non-polar solvents used for Suzuki–Miyaura reactions, closely bound ion pairs. The effects of ion pairing are not described by the continuum model, and would be demanding to account for rigorously. These effects are likely to broadly cancel out when comparing different ligands, so their neglect is unlikely to affect the key conclusions of this work.

3.1.1. Catalyst activation–formation of PdPR$_3$-PhBr

The first step in the catalytic cycle is the formation of the PdPR$_3$-PhBr (**3**) species from Pd(PR$_3$)$_2$ (**1**) and PhBr. This formal substitution process can take place through three different pathways: dissociative, associative and concerted. Most previous computational studies of cross-coupling mechanisms [12,25,29,37–42,76] have assumed that the dissociative mechanism is favoured. In this study, all three pathways have been analyzed with the different phosphines in order to find which one should be favoured. We note that in some computational studies [42,45–50], oxidative addition has been modelled as starting from the diphosphine Pd(0) species itself, without initial loss of phosphine. However, it has been shown that the activation barrier in that case is considerably higher than for the monophosphine case, especially for very bulky phosphines [42]. We have therefore focussed only on the monophosphine pathway. If Suzuki–Miyaura coupling can occur with some phosphines in a bis-phosphine pathway, some of the conclusions about ligand
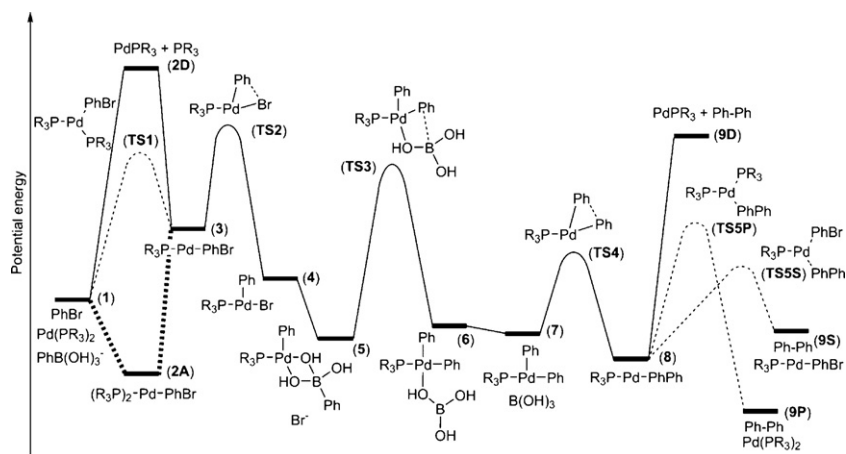
Scheme 3. Generic features of the computed potential energy surface for Suzuki–Miyaura coupling of PhB(OH)$_3^-$ and PhBr catalyzed by Pd(PR$_3$)$_2$. The energies are shown roughly to scale (see Tables 1 and 2 for numerical values).

Table 1
Computed vacuum relative energies, for the species in Scheme 3, in kcal/mol, at the B3LYP level of theory, including corrections for ZPE.

	P^{t}Bu$_3$	P(CF$_3$)$_3$	PMe$_3$	PPh$_3$
1	0.0	0.0	0.0	0.0
2D	31.6	31.5	31.9	31.6
2A	–	−7.7	5.3	7.4
TS1	26.0	22.2	17.6	15.4
3	15.2	9.3	15.5	14.7
TS2	18.4	20.3	19.4	19.0
4	−0.1	5.3	−2.5	−1.4
5	−13.3	−11.9	−20.2	−16.7
TS3	6.5	2.5	−1.9	−0.3
6	−11.2	−17.8	−20.0	−15.9
7	−11.3	−9.9	−11.5	−11.2
TS4	−8.1	−8.1	−6.7	−7.3
8	−46.0	−53.2	−46.1	−46.4
9D	−29.4	−29.5	−29.1	−29.4
TS5P	−32.4	−52.8	−43.5	−43.8
9P	−61.0	−61.0	−61.0	−61.0
TS5S	−34.4	−51.8	−37.8	−37.3
9S	−45.8	−51.7	−45.5	−46.3

effects that we draw here may hence be incorrect, although for the currently popular highly bulky phosphine reactions, our model should be appropriate.

In the dissociative pathway, Pd(PR$_3$)$_2$ would first form the palladium (0) species PdPR$_3$ (**2D**) and PR$_3$, then the former would react with PhBr to yield (**3**). It is known that this direct dissociation is often unfavourable in solution for complexes of the small and medium size phosphines like Pd(PMe$_3$)$_2$ and Pd(PPh$_3$)$_2$ [48]. Indeed, with these ligands, formation of tricoordinated Pd(PR$_3$)$_3$ or even tetracoordinated Pd(PR$_3$)$_4$ is often favourable, and the highly unsaturated monocoordinated PdPR$_3$ species are not expected to form at all readily [77]. We note that the energies for the ligand dissociation (PR$_3$) in the gas phase are very similar for all the studied palladium diphosphines, showing that this endergonic process is practically independent of the ligand nature. Dispersion effects, poorly treated in the present B3LYP calculations [63], might be expected to increase the energy of the dissociated species for the bulkier PPh$_3$ and P^{t}Bu$_3$ cases, hence making the dissociative mechanism less favourable. The coordination of PhBr to PdPR$_3$ (**2D**) is energetically favoured in all cases and the intermediate η^2-PdPR$_3$-PhBr (**3**) is formed through π interaction between the aromatic system of the substrate and the palladium atom [42,78]. There are several possible isomers for the π complex PdPR$_3$–PhBr depending on which carbon atoms in the ring interact to form the η^2 complex.

Table 2
Computed relative energies, for the species in Scheme 3, in kcal/mol, at the B3LYP level of theory, including corrections for ZPE and for solvent effects (THF continuum).

	P^{t}Bu$_3$	P(CF$_3$)$_3$	PMe$_3$	PPh$_3$
1	0.0	0.0	0.0	0.0
2D	27.7	23.8	27.6	27.4
2A	–	−7.2	3.4	10.9
TS1	26.0	22.2	17.2	18.4
3	14.1	8.6	13.9	14.0
TS2	15.5	20.0	15.3	16.9
4	−10.0	0.9	−14.9	−9.7
5	−27.7	−24.0	−36.6	−29.4
TS3	−9.5	−12.0	−20.0	−14.8
6	−25.8	−34.3	−38.6	−31.6
7	−31.6	−27.4	−32.7	−30.1
TS4	−27.6	−25.7	−27.2	−25.7
8	−64.5	−71.1	−65.9	−64.4
9D	−51.0	−54.9	−51.0	−51.3
TS5P	−49.5	−71.0	−61.2	−58.0
9P	−78.7	−78.7	−78.7	−78.7
TS5S	−52.1	−68.8	−55.4	−53.3
9S	−64.6	−70.0	−64.8	−64.7

These isomers are close in energy, and our calculations suggest that the most favourable η^2-interaction is produced with the *meta*- and *para*-C atoms of the ring. The stabilization of η^2-Pd(P(CF$_3$)$_3$)–PhBr is around 5–6 kcal/mol greater than for the other phosphines, perhaps due to the weaker *trans*-influence of the very electron-poor ligand [79].

The associative pathway consists of sequential coordination of PhBr to Pd(PR$_3$)$_2$ followed by PR$_3$ dissociation. The tricoordinated species Pd(PR$_3$)$_2$–PhBr (**2A**) have been found in previous computational studies for PMe$_3$ and PPh$_3$ [80]. Several limiting variations on this mechanism are possible in principle, depending on the stability of the intermediate tricoordinated species and on whether the ligand addition and loss steps occur through barrierless processes or through marked transition states on the potential energy surface. As noticed elsewhere [42], in the case of P^{t}Bu$_3$, it was impossible to find the tricoordinated species Pd(P^{t}Bu$_3$)$_2$–PhBr; this complex appears to be unstable due to steric reasons and all attempts to locate a corresponding structure by geometry optimization led to dissociation of PhBr. This is not unexpected given the large cone angle (182°) of the P^{t}Bu$_3$ ligand [66], which effectively shields all of the coordination sphere of Pd in Pd(P^{t}Bu$_3$)$_2$; as a result the associative pathway seems to be impossible for this bulky phosphine. For the rest of the ligands, the tricoordinated species (**2A**) of Pd(PMe$_3$)$_2$, Pd(P(CF$_3$)$_3$)$_2$ and Pd(PPh$_3$)$_2$ were found. These complexes show that a π-bond is formed between the palladium atom and the aromatic ring of PhBr. In all cases the favoured isomer for this η^2-interaction involves coordination of the *ipso*- and *ortho*-aromatic carbons. The tricoordinated complex is more stable than the starting materials (−7.7 kcal/mol) for P(CF$_3$)$_3$, and it is therefore possible that PhBr addition to Pd(P(CF$_3$)$_3$)$_2$ may be barrierless (we have not explored this possible TS). The big difference in energy between this species and PdP(CF$_3$)$_3$–PhBr (**3**) indicates that the phosphine loss is very endothermic. In the case of PMe$_3$ and PPh$_3$, the tricoordinated (**2A**) species are slightly less stable than the reactants (5.3 and 7.4 kcal/mol, respectively). This implies that there must be at least a small potential energy barrier for addition of PhBr; again, we have not explored this TS. Again, phosphine loss from these adducts is endothermic, and may involve a barrier on the potential energy surface, though we have not verified this.

In a hypothetical concerted pathway, dissociation of PR$_3$ occurs in the same elementary step as addition of PhBr. This mechanism can be viewed as involving stabilization of the developing unsaturated PdPR$_3$ species by the π system of the aryl halide. This process, although endergonic, provides a lower energy pathway, at least in terms of potential energy, than the direct dissociative pathway. We have located TSs for this process for all phosphines. In each case, the TSs have structures with a long distance between the Pd and the dissociating PR$_3$ and a short Pd–πPhBr distance. This means that it is difficult to state with confidence whether these TSs are direct substitution TSs, or TSs for loss of phosphine from the associative adducts (**2A**). At least for the case of P^{t}Bu$_3$, however, where there is no stable adduct (**2A**), (**TS1**) must be a substitution TS. In the other cases, it is the highest barrier along a substitution process with associative character, and the distinction is hence not so important. The height of the barrier for this transition state seems to depend markedly on the identity of the ligand, but it is difficult at first sight to explain the relationship.

This TS has been located previously in the case of P^{t}Bu$_3$ [42], for substitution by PhBr or PhCl. These authors however discounted this TS, as it lies higher in free energy than species (**2D**). Our results in Table 1 and Scheme 3 suggest that (**TS1**) is favoured over dissociation into (**2D**), but it could be claimed that this is an artefact arising due to our choice to focus on potential energies, and thereby not to include the entropic penalty associated with binding the aryl halide before loss of phosphine. Nevertheless, we believe that the concerted mechanism is, at least under certain conditions, com-

petitive with the dissociative mechanism, as we have previously reported experimental observations for a related Pd-based catalytic cycle that can only be rationalised in this way [43]. It is possible that the calculations of Ref. [42] overestimate the energy of (**TS1**) due to the neglect of dispersion interactions [63].

In conclusion to this section, we consider that both the fully dissociative and the partially associative concerted pathways should be considered as possible for formation of PdPR₃–ArX intermediates in Suzuki–Miyaura cross-coupling. These are the only possible mechanisms in the case of P^{t}Bu₃, as with this phosphine, formation of the tricoordinated complex necessary to follow the stepwise associative process is not possible. In the case of the PPh₃, PMe₃ and P(CF₃)₃ ligands, this third mechanism, less thoroughly explored here, may also be possible, and indeed, all three mechanisms are difficult to discriminate between in energy terms.

3.1.2. Oxidative addition

The oxidative addition of aryl bromides is a very common step in cross-coupling reactions and it has been studied thoroughly, experimentally and computationally [41,42,44–50]. In this process the palladium atom is inserted in the C_{Ar}–Br bond in (**3**), leading to the formation of the T-shaped species (**4**) where the bromine and the phosphine lie *trans* to each other due to the higher *trans*-influence of the Ph group and the steric bulk of the larger phosphines. It is possible that with the smaller phosphines, addition leads to another isomer initially, with aryl and phosphine lying *trans* to one another, but the barrier to rearrangement should be small. In the case of P^{t}Bu₃, the vacant coordination site *trans* to the aryl group is occupied by an agostic interaction with a γ-C–H bond of the phosphine [37,81,82]. The computed Pd–H and C–H distances are 2.467 and 1.101 Å (vs 1.093 Å on average for the non-agostic C–H bonds of the P^{t}Bu₃ ligand). This weak interaction has been observed also in crystal structures [81] and its effect in stabilizing low coordinate palladium complexes has been studied computationally [82]. For the rest of the studied phosphines, where no agostic interaction can be established, stabilization of the low coordinated palladium (II) can only be achieved by the formation of halide-bridged dimers [82–84] or addition of solvent or other species in the vacant coordination site, a process that we have not examined here.

The three-membered oxidative addition transition state (**TS2**) is very similar in structure for all the phosphines; the C_{Ar}–Br distance is around 0.3 Å longer than in PhBr. As expected, the oxidative addition (**3**) → (**TS2**) barrier is lower for the electron-rich phosphines P^{t}Bu₃, PMe₃ and PPh₃ (3.2, 3.9 and 4.2 kcal/mol, respectively); and higher (11 kcal/mol) for the electron-poor P(CF₃)₃ [85].

3.1.3. Substitution of Br⁻ by PhB(OH)₃⁻

In this step of the catalytic cycle the bromine atom of intermediate (**4**) is displaced by the hydroxyboronate anion PhB(OH)₃⁻. The latter species can be formed from the reactant organoboronic acid PhB(OH)₂ in the presence of base and traces of water, in a facile process that we do not investigate here. Addition of hydroxide to the boronic acid has been shown to be practically barrierless [17].

The detailed mechanism of this ligand exchange has been suggested to be stepwise, consisting of initial weak interaction between the hydroxyboronate and the intermediate (**4**) to form a complex, followed by an exchange step via a transition state to produce the intermediate (**5**), and finally loss of bromide [86]. In this work, these steps have not been studied thoroughly as we expect that the barrier of this process is not going to contribute significantly to the observed reactivity. In the square planar species formed after the ligand exchange (**5**), the PhB(OH)₃⁻ ligand acts as a chelate, with two of the hydroxyl groups acting as donor groups to the palladium. Due to the difference in *trans*-influence between Ph and PR₃, all these species present distorted square planar geometries, where the Pd–O distances are slightly longer for

the substituents *trans* to the aryl group; besides, the bond angles C_{Ar}–Pd–O are always smaller (around 160°) than those of P–Pd–O (∼170°).

3.1.4. Transmetallation

This step involves the transfer of the phenyl group from the coordinated hydroxyboronate to the palladium atom. It has been stated that PhB(OH)₃⁻ is a much better transmetallating agent than the starting boronic acid PhB(OH)₂ [18]; the quaternization of the boron with a negatively charged base enhances the nucleophilicity of the aryl group and facilitates its migration to the palladium [4]. Accordingly, we have not investigated this process using a boronic acid ligand to palladium.

In the transmetallation mechanism as modelled here, the metal centre is bound to only one phosphine, but the palladium centre in the starting complex (**5**) is nevertheless tetracoordinate and square planar due to the chelating nature of boronate. Transmetallation requires that one of the Pd–O bonds of (**5**) is cleaved in order to generate a free site for the new Pd–C_{Ar} bond. It is known that the *trans*-influence of the Ph group is higher than that for the phosphine and so the Pd–O bond trans to the Ph should be more reactive, thereby naturally leading to the more stable isomer of (**6**) in which the two phenyl groups lie *cis* to one another. In (**TS3**) for transmetallation that we have characterized, the Pd–O interaction *trans* to phosphine is broken, and conformational reorientation of the boronate has brought the transferring phenyl group close to Pd.

The four-membered ring transition state (**TS3**) shows the same general structure for all the phosphines, with the Pd–C_{Ar} distances around 2.2 Å, and the B–C_{Ar} distances ca. 0.4 Å longer than those in (**5**). There is some evidence that under some conditions, this step can be rate limiting (competing with the ligand dissociation) and so, the barriers for the (**5**) → (**TS3**) transformation were expected to be quite high. Surprisingly, this behaviour is not really confirmed, with all the computed barriers found to be less than 20 kcal/mol. One way to explain this discrepancy is that it is possible that with the less bulky ligands, the oxidative addition product (**3**) adds a second phosphine, so that transmetallation through (**TS3**) requires initial loss of phosphine, adding to the barrier. The barriers as described here for the electron-rich ligands P^{t}Bu₃ and PMe₃ (barriers of 19.8 and 18.4 kcal/mol, respectively) are found to be slightly higher than those for the electron-poorer ligands PPh₃ and P(CF₃)₃ (16.4 and 14.4 kcal/mol, respectively), indicating that the ligand electronics seem to be very important in this step of the catalytic cycle. This kind of electronic dependency has never been associated to a transmetallation barrier before.

3.1.5. Loss of B(OH)₃

After the transmetallation, the boric acid B(OH)₃ formed remains bonded to palladium through one of the oxygen atoms, in a position *trans* to one of the Ph groups, in the complex (**6**). However, the boric acid is a weak ligand, especially given the strong *trans*-influence of the phenyl group, so the Pd–O bond strength is small and B(OH)₃ can readily dissociate to form the T-shaped species (**7**), in which the two phenyl groups again remain *cis* to each other. As explained for (**4**), this formally tricoordinate species can involve stabilization of the low coordinated palladium (II) center in a variety of ways, e.g. formation of halide-bridged dimers [82–84]. In the case of P^{t}Bu₃, agostic interaction between the palladium and one γ-C–H bond of the phosphine is re-established [37,81,82], as shown in Fig. 1; this fact can also explain why the loss of B(OH)₃ seems to be energetically favoured for P^{t}Bu₃ and unfavoured for the rest of studied phosphines.

3.1.6. Reductive elimination

In this step, a bond between the two phenyl groups attached to the metal is formed producing biphenyl (**9**) which is the cou-
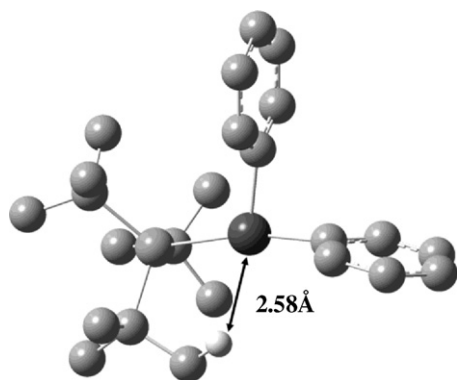
Fig. 1. Agostic interaction observed in complex (**7**) between the palladium atom and one γ-C–H bond of P^{t}Bu$_3$ (other H atoms have been omitted for clarity).

pling product. It has been stated that for the reductive elimination to happen, the two eliminating groups have to be *cis* to each other [57]; in this case, the two phenyl groups in intermediate (**7**) are already *cis*, so no rearrangement is needed prior to elimination. The three-membered transition state (**TS4**) has a C_{Ar}–C_{Ar} distance of around 2.2 Å, and Pd–C_{Ar} distances that are only slightly longer than in (**7**). These small changes in the geometry are consistent with the low barriers found for this step of the reaction: 4.7, 1.7, 3.9 and 3.2 kcal/mol for PMe$_3$, P(CF$_3$)$_3$, PPh$_3$ and P^{t}Bu$_3$, respectively (Table 1). It is known that electron-poor ligands and sterically hindered ligands tend to lower this barrier [87]; as can be seen, the lowest barrier is found for P(CF$_3$)$_3$. Among the electron-rich ligands P^{t}Bu$_3$ has a lower barrier than PMe$_3$ due to its higher bulkiness.

After the reductive elimination, the formed biphenyl remains attached to the palladium monophosphine through an interaction between an aromatic ring and the palladium atom, η^2-PdPR$_3$–PhPh (**8**), similar to the one described for intermediate (**3**). In this case, the most favoured η^2-interaction is achieved with the *ortho-* and *meta-*C atoms of one of the biphenyl rings.

3.1.7. Regeneration of the catalyst—product release

This is the last step of the reaction; the biphenyl product is released from (**8**) and the active catalyst is recovered, closing the catalytic cycle. This process, just as seen for the catalyst activation, can take place through several different pathways: dissociative, associative or concerted; but in this case, it is even more complicated as the associative and concerted pathways can be mediated by the substrate PhBr or by a free phosphine PR$_3$. As shown in a previous experimental and computational study of the Newman–Kwart reaction [43], it is important to consider the nature of the steps leading to product removal and renewed formation of the aryl bromide complex. This is because they can have a large influence on the overall turnover rate, and the effect of added phosphine on turnover.

In the dissociative pathway, the π interaction in the complex η^2-PdPR$_3$–PhPh (**8**) is broken to form biphenyl (**9D**) and the palladium monophosphine PdPR$_3$, which will take the catalytic cycle back to (**2D**). This process is endergonic for all the ligands, around 17 kcal/mol for the electron-rich phosphines PMe$_3$, PPh$_3$ and P^{t}Bu$_3$, and 23 kcal/mol for P(CF$_3$)$_3$.

The associative pathways are putative sequential processes, in which initial addition of PhBr or a phosphine PR$_3$ to (**8**) gives the tricoordinated species η^2-PhPh–PdPR$_3$–η^2-PhBr or η^2-Pd(PR$_3$)$_2$–PhPh, respectively. In the second step, biphenyl would then dissociate to regenerate η^2-PdPR$_3$–PhBr (**3**) or Pd(PR$_3$)$_2$ (**1**). Our attempts to characterize these tricoordinate adducts were unsuccessful; during geometry optimization, one of the ligands: PhBr, PhPh or PR$_3$ was found to dissociate from the metal. Although

this behaviour was expected for the bulky P^{t}Bu$_3$-derived species, it was more surprising for the other phosphines given the existence as local minima of the analogous (**2D**) species. In any case, this suggests that associative displacement of product from (**8**) can be neglected.

In the concerted pathways the product is displaced from (**8**) by a free phosphine PR$_3$ or substrate PhBr to release biphenyl (**9S** or **9P**) and PdPR$_3$–PhBr (**3**) or Pd(PR$_3$)$_2$ (**1**), respectively. The structure of the transition states (**TS5P**) leading to (**9P**) is, as could be expected, similar to the ones found for (**TS1**), with a long distance between the palladium atom and the entering phosphine and a short distance between the metal and the leaving biphenyl group. The early nature of the TSs is consistent with the exothermic nature of the step. On the other hand, the transition states (**TS5S**) show that the Pd–PhPh and Pd–PhBr distances are similar, again consistent with a reaction that involves an overall small energy change. The tricoordinated transition states, (**TS5P**) and (**TS5S**), are always lower in energy than the direct dissociation for all the phosphines so this pathway will be preferred. Indeed, for the P^{t}Bu$_3$ ligand, (**TS5S**), which leads directly back into the catalytic cycle, is slightly lower in energy than (**TS5P**) which regenerates the 'blocked' diphosphine species. This suggests that small amounts of added phosphine may not be able to inhibit catalytic turnover, despite the fact that the active species involve only one phosphine ligand. This behaviour is similar to that found computationally – and experimentally – in the recently developed catalytic version of the Newman–Kwart reaction [43]. For the other ligands, these two TSs lie in the opposite order in terms of their relative energy. This may be one of the reasons why electron-rich bulky ligands are good catalysts for this reaction [7], as they favour regeneration of (**3**) without requiring initial phosphine dissociation. Another favourable aspect of bulky phosphines, not examined here, is that they may help to avoid sequestration of the active palladium species by dimerization of the tricoordinated intermediates along the cycle which seems to be one of the principal experimental problems for the smaller phosphines [82–84].

Another more general point can be made about this behaviour, together with the previous discussion of the concerted process through (**TS1**) for formation of (**3**) by concerted substitution of ligand by substrate in Pd(P^{t}Bu$_3$)$_2$. It was already known that the mono substituted species PdPR$_3$ is rather unstable, and that it readily forms adducts with various molecules [19]. However, it is also known that monoligated PdPR$_3$ is much more active in oxidative addition (and reductive elimination) than doubly ligated palladium. The present mechanisms suggest that it is possible to form catalytically competent mono ligated species without ever forming the unstable PdPR$_3$.

3.2. Quantitative ligand effects on the barriers in the Suzuki–Miyaura coupling

Recently [67–70], it has been found that the use of statistical analysis can be used to improve the understanding of ligand effects on calculated properties such as bonding energies or energy barriers. In this work we have built multiple linear regression models to predict the DFT calculated energy barriers for some of the key steps of the Suzuki–Miyaura reaction in terms of the phosphine electronic and steric features. Usually, phosphine ligand electronics and sterics are described using the Tolman parameters [66] and they have been already used in quantitative statistical ligand effect studies [70]. In this work the phosphine ligand electronic and steric features are described by different descriptors, included in our Ligand Knowledge Base [68]. The use of a broader set of descriptors provides a more detailed overview of ligand properties [67]. Electronic properties of ligands can be captured by several descriptors, including the energies of the molecular frontier orbitals HOMO and LUMO. These descriptors roughly account for electron σ-donation

Table 3
DFT barriers and descriptors used in the regression models.

		P^{t}Bu$_3$	P(CF$_3$)$_3$	PMe$_3$	PPh$_3$
Barrier (kcal/mol)	Oxidative addition	3.2	11.0	3.9	4.3
	Transmetallation	19.8	14.4	18.3	16.4
	Reductive elimination	3.2	1.7	4.7	3.9
Descriptor	HOMO (Hartree)	−0.173	−0.277	−0.190	−0.187
	LUMO (Hartree)	0.028	−0.058	0.033	−0.051
	He$_8$_steric (kcal/mol)	23.4	3.0	3.0	8.0
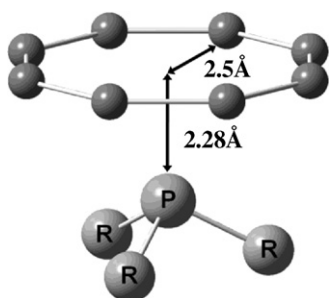
Fig. 2. Geometry used for the computation of the He$_8$_steric parameter.

and π-acceptance properties of the phosphines, respectively. On the other hand, ligand sterics can be described using several values, including the He$_8$_steric parameter, calculated as the interaction energy between the phosphine ligand and a fixed ring of eight helium atoms [68]. This set-up (Fig. 2) mimics the interactions between a ligand and other *cis*-coordinated groups in an octahedral complex.

A variety of simple multilinear regression models were constructed for the DFT energy barriers of the oxidative addition, transmetallation and reductive elimination steps. Encouragingly, some fairly successful models were found that use physically plausible descriptors as input, namely the He$_8$_steric descriptor and the energy of the HOMO or the LUMO mentioned above. The values of the studied DFT barriers and the HOMO, LUMO and He$_8$_steric descriptors for each phosphine are shown in Table 3.

The standardized regression coefficients (β_i) for the descriptors in each of the model provide information as to the relative importance of each descriptor in the correlations derived here. The sign of each standardized regression coefficient indicates whether an increase in a given descriptor leads to an increase (positive) or decrease (negative) in the predicted barrier height. The standardized regression coefficients for the three multilinear regression models, together with the associated determination coefficient (R^2), are shown in Table 4. In the case of the transmetallation step, two different models were constructed, as shown.

It should be noted that a rather small dataset is used here (only four ligands), which clearly limits the statistical significance of the models. However, the models are quite simple, and are physically plausible, which suggests that they do already provide valuable quantitative insight into the ligand effects on each barrier.

Table 4
Standardized regression coefficients for the multivariate models used to reproduce DFT-calculated energy barriers. In the case of transmetallation, two different models (a) and (b) are shown, as discussed in the text.

Barrier	R^2	β_{HOMO}	β_{LUMO}	β_{He_8}
Oxidative addition	0.996	−3.76	–	0.23
Transmetallation (a)	0.820	1.61	–	0.72
Transmetallation (b)	0.943	–	1.72	0.90
Reductive elimination	0.972	1.52	–	−0.91

3.2.1. Oxidative addition

The height of this barrier has been calculated as the energy difference between η^2-PdPR$_3$–PhBr (**3**) and the corresponding oxidative addition transition state (**TS2**) rather than from the diphosphine Pd(PR$_3$)$_2$ reactant because we have assumed that this process will always take place after the phosphine dissociation. It is known [85] that strong σ-donor ligands favour palladium insertion into the C$_{Ar}$–X bonds and it is therefore no surprise that a higher oxidative addition barrier is found for the electron-poor P(CF$_3$)$_3$ than for the electron-rich ligands P^{t}Bu$_3$, PMe$_3$ and PPh$_3$. The multilinear regression model obtained using the HOMO energy and the He$_8$_steric descriptors, Table 4, shows that the oxidative addition barrier is mainly governed by the phosphine electronics; the standardized coefficient of the HOMO ($\beta_{HOMO} = -3.76$) is more than sixteen times larger than for the He$_8$_steric descriptor ($\beta_{He_8} = 0.23$). The direct regression of the barrier heights with the HOMO energy gives a very good model with a determination coefficient $R^2 = 0.990$, confirming that the ligand steric features are far less important in the oxidative addition barrier than the electron donation ability. In both cases the β_{HOMO} coefficient is negative indicating that the stronger σ-donor ligands, with higher energy HOMOs, will produce lower oxidative addition barriers, in agreement with what has been published previously [85].

3.2.2. Transmetallation

The transmetallation barrier is calculated as the energy needed to produce the (**5**) → (**TS3**) transformation; in this step the Ph group of PhB(OH)$_3^-$ is transferred to the palladium atom. As the quaternization of the boronic acid enhances the nucleophilicity of the aryl group [4], this step can be seen as a nucleophilic attack of the Ph of PhB(OH)$_3^-$ on the square planar palladium complex (**5**). Although this is one of the key steps of the Suzuki–Miyaura coupling, it has not been explored as thoroughly as other steps, i.e. oxidative addition, probably because the mechanism of transmetallation depends upon the organometallic reagent in question [1]. As a result, we could not find any analysis of ligand effects on the transmetallation barrier of the Suzuki–Miyaura coupling in the literature and therefore we cannot compare the results obtained with the regression model to any experimental or calculated data. The first regression model for this process, built using the HOMO energy and the He$_8$_steric descriptors, is not very good ($R^2 = 0.820$), Table 4. This can be related to the fact that the HOMO energy descriptor is not well suited to describe this step. In the transmetallation the palladium atom is attacked by the electron-rich Ph group of the boronate and it is therefore not surprising that using a descriptor that accounts for electron σ-donation provides a poor model.

In the second model, which uses the LUMO energy and the He$_8$_steric parameter as predictor variables, a much improved regression model is obtained ($R^2 = 0.943$), Table 4, as could be expected. In this case, the standardized coefficients confirm that both descriptors are significant for the correlation ($\beta_{LUMO} = 1.72$ and $\beta_{He_8} = 0.90$); with the steric factor twice as important as the electronic features. The sign of the He$_8$_steric parameter is positive, which means that bulkier ligands will produce higher barriers for the transmetallation. The rearrangement of the bonded boronate

prior to the transmetallation may be responsible for this, as it can be expected that this process should be more difficult for the bulkier phosphines. The LUMO energy descriptor also has a positive sign, indicating that the better π-acceptor phosphines will contribute to lowering the transmetallation barrier, as they can better stabilize the developing additional electron density on the metal.

3.2.3. Reductive elimination

This barrier is calculated as the difference in energy between Ph-PdPR$_3$-Ph (**7**) and the corresponding reductive elimination transition state (**TS4**). It has been stated that bulky and electron-poor ligands contribute to lowering this barrier [87]. A very good linear model ($R^2 = 0.972$) can be built using the HOMO energy and the He$_8$_steric descriptors, Table 4. The standardized coefficients of the HOMO ($\beta_{HOMO} = 1.52$) and the He$_8$_steric descriptor ($\beta_{He_8} = -0.91$) indicate that both factors are important in the reductive elimination. The sign of β_{HOMO} is positive which means that strong σ-donor ligands such as P^{t}Bu$_3$ and PMe$_3$ will make this barrier higher whereas weak σ-donors like P(CF$_3$)$_3$ will lower it. As expected, β_{He_8} is negative, indicating that the bulky phosphines will lower the reductive elimination barrier; as bigger ligands will push the two phenyl groups closer it will be easier to form the biphenyl product. The relative importance of both descriptors shows that electronics play a bigger role in the reductive elimination than the sterics, which is consistent with the fact that this process occurs starting from the relatively unhindered monoligated palladium phosphine species.

4. Conclusions

The full catalytic cycle of the Suzuki–Miyaura reaction between phenyl bromide and PhB(OH)$_3$$^-$ has been studied using four different palladium monophosphine catalysts, derived from Pd(PMe$_3$)$_2$, Pd(P(CF$_3$)$_3$)$_2$, Pd(PPh$_3$)$_2$ and Pd(P^{t}Bu$_3$)$_2$. The three possible activation pathways of the catalyst, by losing one of the phosphines in an associative, dissociative or concerted mechanism, have been studied. Our calculations suggest that all of them may occur in competition with one another, except in the case of P^{t}Bu$_3$, where the bulkiness of the ligand prevents the formation of Pd(P^{t}Bu$_3$)$_2$–PhBr and thus forces the reaction to follow the dissociative or concerted pathways. We note that it is possible that substitution of PR$_3$ by PhBr could be overall rate-limiting for oxidative addition, a fact that would explain the observation in some cases of a rate-limiting step prior to ligand loss in reactions of Pd(PR$_3$)$_2$ with ArX [38,50,51,88]. The present calculations, which do not account for dispersion or entropic effects, are however not able to make predictions on this question.

Similar conclusions to those given above for the catalyst activation step could have been expected in the step where the catalyst is regenerated; unfortunately, the tricoordinated Pd(P^{t}Bu$_3$)$_2$–PhPh species could not be found for any of the phosphines and the associative pathways could not be studied. Even so, a difference between the ligands is found in the concerted catalyst regenerations, for PMe$_3$, P(CF$_3$)$_3$ and PPh$_3$ the substitution of the biphenyl product by PR$_3$ is favoured whereas for P^{t}Bu$_3$ the displacement of the product is more likely to be achieved by PhBr. These concerted substitutions will take the reaction back to Pd(PMe$_3$)$_2$, Pd(P(CF$_3$)$_3$)$_2$, Pd(PPh$_3$)$_2$ and Pd(P^{t}Bu$_3$)–PhBr, respectively; making P^{t}Bu$_3$ the better catalyst as it will avoid the highly endergonic phosphine dissociation step.

Also, multiple linear regression models have been constructed to quantitatively analyze the ligand effects of the different phosphines on the oxidative addition, transmetallation and reductive elimination energy barriers. As it has been stated before, the oxidative addition is mainly dominated by ligand electronics; in this case the HOMO descriptor, used to account for the phosphine σ-donation, is far more important than the He$_8$_steric parameter. The sign of the HOMO regression coefficient confirms that the better σ-donor ligands will lead to lower oxidative addition barriers. The computed energy barriers for the transmetallation show that this step is strongly influenced by the ligand, with the electron-poor ligand P(CF$_3$)$_3$ providing the lowest value for this transformation. This is one of the key new observations in this work. The multilinear regression model built to predict these barriers indicates that both ligand electronic and steric features are important. Bigger ligands tend to increase this energy barrier due to possible interactions with the rest of the substituents on the palladium during the structural rearrangement that takes place during this step. On the other hand, better π-acceptor ligands lower the transmetallation barrier as they are able to accommodate the incoming electron density developing as a result of the nucleophilic attack of the boronate phenyl group on the palladium atom. The analysis of ligand effects on the low reductive elimination barrier shows that both sterics and electronics are significant. The multilinear regression model indicates that weak σ-donors and bulky ligands will produce the lower barriers for this step.

Appendix A. Supplementary data

Supplementary data associated with this article can be found, in the online version, at doi:10.1016/j.molcata.2010.02.021.

References

[1] N. Miyaura, A. Suzuki, Chem. Rev. 95 (1995) 2457–2483.
[2] J.P. Wolfe, R.A. Singer, B.H. Yang, S.L. Buchwald, J. Am. Chem. Soc. 121 (1999) 9550–9561.
[3] A.F. Littke, G.C. Fu, Angew. Chem. Int. Ed. 41 (2002) 4176–4211.
[4] N. Miyaura, J. Organomet. Chem. 653 (2002) 54–57.
[5] M.R. Netherton, G.C. Fu, Adv. Synth. Catal. 346 (2004) 1525–1532.
[6] H. Doucet, Eur. J. Org. Chem. 2008 (2008) 2013–2030.
[7] R. Martin, S.L. Buchwald, Acc. Chem. Res. 41 (2008) 1461–1473.
[8] M. Thimmaiah, X. Zhang, S. Fang, Tetrahedron Lett. 49 (2008) 5605–5607.
[9] S.D. Dreher, S.-E. Lim, D.L. Sandrock, G.A. Molander, J. Org. Chem. 74 (2009) 3626–3631.
[10] G.A. Molander, B. Canturk, Angew. Chem. Int. Ed. 48 (2009) 9240–9261.
[11] A. Rudolph, M. Lautens, Angew. Chem. Int. Ed. 48 (2009) 2656–2670.
[12] T.E. Barder, S.D. Walker, J.R. Martinelli, S.L. Buchwald, J. Am. Chem. Soc. 127 (2005) 4685–4696.
[13] I.N. Francesco, A. Wagner, F. Colobert, Eur. J. Org. Chem. 2008 (2008) 5692–5695.
[14] Y.L. Choi, C.-M. Yu, B.T. Kim, J.-N. Heo, J. Org. Chem. 74 (2009) 3948–3951.
[15] M.G. Organ, S. Çalimsiz, M. Sayah, K.H. Hoi, A.J. Lough, Angew. Chem. Int. Ed. 48 (2009) 2383–2387.
[16] Y. Uozumi, Y. Matsuura, T. Arakawa, Y.M.A. Yamada, Angew. Chem. Int. Ed. 48 (2009) 2708–2710.
[17] A.A.C. Braga, N.H. Morgon, G. Ujaque, F. Maseras, J. Am. Chem. Soc. 127 (2005) 9298–9307.
[18] A.A.C. Braga, N.H. Morgon, G. Ujaque, A. Lledós, F. Maseras, J. Organomet. Chem. 691 (2006) 4459–4466.
[19] A.A.C. Braga, G. Ujaque, F. Maseras, Organometallics 25 (2006) 3647–3658.
[20] Y.-L. Huang, C.-M. Weng, F.-E. Hong, Chem. Eur. J. 14 (2008) 4426–4434.
[21] C. Gourlaouen, G. Ujaque, A. Lledós, M. Medio-Simon, G. Asensio, F. Maseras, J. Org. Chem. 74 (2009) 4049–4054.
[22] W. Shen, Tetrahedron Lett. 38 (1997) 5575–5578.
[23] A. Zapf, A. Ehrentraut, M. Beller, Angew. Chem. 39 (2000) 4153–4155.
[24] J.H. Kirchhoff, M.R. Netherton, I.D. Hills, G.C. Fu, J. Am. Chem. Soc. 124 (2002) 13662–13663.
[25] U. Christmann, R. Vilar, Angew. Chem. Int. Ed. 44 (2005) 366–374.
[26] C.A. Fleckenstein, H. Plenio, Chem. Eur. J. 13 (2007) 2701–2716.
[27] C.A. Fleckenstein, H. Plenio, J. Org. Chem. 73 (2008) 3236–3244.
[28] G.C. Fu, Acc. Chem. Res. 41 (2008) 1555–1564.
[29] S.D. Walker, T.E. Barder, J.R. Martinelli, S.L. Buchwald, Angew. Chem. Int. Ed. 43 (2004) 1871–1876.
[30] B. Saito, G.C. Fu, J. Am. Chem. Soc. 129 (2007) 9602–9603.

[31] C.W.K. Gstöttmayr, V.P.W. Böhm, E. Herdtweck, M. Grosche, W.A. Herrmann, Angew. Chem. Int. Ed. 41 (2002) 1363–1365.
[32] G. Altenhoff, R. Goddard, C.W. Lehmann, F. Glorius, Angew. Chem. Int. Ed. 42 (2003) 3690–3693.
[33] G. Altenhoff, R. Goddard, C.W. Lehmann, F. Glorius, J. Am. Chem. Soc. 126 (2004) 15195–15201.
[34] E. Assen, B. Kantchev, C.J. O'Brien, M.G. Organ, Angew. Chem. Int. Ed. 46 (2007) 2768–2813.
[35] C.S. Linninger, E. Herdtweck, S.D. Hoffmann, W.A. Herrmann, F.E. Kühn, J. Mol. Struct. 890 (2008) 192–197.
[36] N. Marion, S.P. Nolan, Acc. Chem. Res. 41 (2008) 1440–1449.
[37] J.P. Stambuli, M. Buhl, J.F. Hartwig, J. Am. Chem. Soc. 124 (2002) 9346–9347.
[38] F. Barrios-Landeros, J.F. Hartwig, J. Am. Chem. Soc. 127 (2005) 6944–6945.
[39] C.J.-C. Lee, F.-E. Hong, Organometallics 24 (2005) 5686–5695.
[40] L.J. Goossen, D. Koley, H.L. Hermann, W. Thiel, Organometallics 25 (2006) 54–67.
[41] M. Ahlquist, P.-O. Norrby, Organometallics 26 (2007) 550–553.
[42] Z. Li, Y. Fu, Q.-X. Guo, L. Liu, Organometallics 27 (2008) 4043–4049.
[43] J.N. Harvey, J. Jover, G.C. Lloyd-Jones, J.D. Moseley, P. Murray, J.S. Renny, Angew. Chem. Int. Ed. 48 (2009) 7612–7615.
[44] J.F. Hartwig, F. Paul, J. Am. Chem. Soc. 117 (1995) 5373–5374.
[45] A.L. Casado, P. Espinet, Organometallics 17 (1998) 954–959.
[46] E. Galardon, S. Ramdeehul, J.M. Brown, A. Cowley, K.K.M. Hii, A. Jutand, Angew. Chem. Int. Ed. 41 (2002) 1760–1763.
[47] L.J. Goossen, D. Koley, H.L. Hermann, W. Thiel, Organometallics 24 (2005) 2398–2410.
[48] K.C. Lam, T.B. Marder, Z. Lin, Organometallics 26 (2006) 758–760.
[49] R. Fazaeli, A. Ariafard, S. Jamshidi, E.S. Tabatabaie, K.A. Pishro, J. Organomet. Chem. 692 (2007) 3984–3993.
[50] F. Barrios-Landeros, B.P. Carrow, J.F. Hartwig, J. Am. Chem. Soc. 131 (2009) 8141–8154.
[51] C. Amatore, A. Jutand, Acc. Chem. Res. 33 (2000) 314–321.
[52] A.O. Aliprantis, J.W. Canary, J. Am. Chem. Soc. 116 (2002) 6985–6986.
[53] Y. Nishihara, H. Onodera, K. Osakada, Chem. Commun. (2004) 192–193.
[54] M. Sumimoto, N. Iwane, T. Takahama, S. Sakaki, J. Am. Chem. Soc. 126 (2004) 10457–10471.
[55] M.L. Clarke, M. Heydt, Organometallics 24 (2005) 6475–6478.
[56] V.P. Ananikov, D.G. Musaev, K. Morokuma, J. Am. Chem. Soc. 124 (2002) 2839–2852.
[57] A. Gillie, J.K. Stille, J. Am. Chem. Soc. 102 (1980) 4933–4941.
[58] E. Zuidema, P.W.N.M. van Leeuwen, C. Bo, Organometallics 24 (2005) 3703–3710.
[59] J.F. Hartwig, Inorg. Chem. 46 (2007) 1936–1947.
[60] L.J. Goossen, D. Koley, H.L. Hermann, W. Thiel, J. Am. Chem. Soc. 127 (2005) 11102–11114.
[61] M. Ahlquist, P. Fristrup, D. Tanner, P.-O. Norrby, Organometallics 25 (2006) 2066–2073.
[62] A.C. Tsipis, O.A. Guy, J.N. Hervey, Dalton Trans. (2005) 2849–2858.
[63] Y. Minenkov, G. Occhipinti, V.R. Jensen, J. Phys. Chem. A 113 (2009) 11833–11844.
[64] N. Sieffert, M. Bühl, Inorg. Chem. 48 (2009) 4622–4624.
[65] Y. Zhao, D.G. Truhlar, J. Chem. Theory Comput. 5 (2009) 324–333.
[66] C.A. Tolman, Chem. Rev. 77 (1977) 313–348.
[67] N. Fey, A.G. Orpen, J.N. Harvey, Coord. Chem. Rev. 253 (2009) 704–722.
[68] N. Fey, A.C. Tsipis, S.E. Harris, J.N. Harvey, A.G. Orpen, R.A. Mansson, Chem. Eur. J. 12 (2006) 291–302.
[69] G. Occhipinti, H.-R. Bjorsvik, V.R. Jensen, J. Am. Chem. Soc. 128 (2006) 6952–6964.
[70] M. Sparta, K.J. Borve, V.R. Jensen, J. Am. Chem. Soc. 129 (2007) 8487–8499.
[71] Jaguar v. 6.0, Schrödinger LLC, New York, NY, 2005.
[72] J.N. Harvey, Faraday Discuss. 145 (2010) 487–505, and references cited.
[73] D.J. Tannor, B. Marten, R. Murphy, R.A. Friesner, D. Sitkoff, A. Nicholls, B. Honig, M. Ringnalda, W.A. Goddard, J. Am. Chem. Soc. 116 (1994) 11875–11882.
[74] B. Marten, K. Kim, C. Cortis, R.A. Friesner, R.B. Murphy, M.N. Ringnalda, D. Sitkoff, B. Honig, J. Phys. Chem. 100 (1996) 11775–11788.
[75] H.M. Senn, T. Ziegler, Organometallics 23 (2004) 2980–2988.
[76] A. Ariafard, B.F. Yates, J. Am. Chem. Soc. 131 (2009) 13981–13991.
[77] C. Amatore, F. Pfluger, Organometallics 9 (1990) 2276–2282.
[78] L.J. Goossen, D. Koley, H.L. Hermann, W. Thiel, Chem. Commun. (2004) 2141–2143.
[79] F.R. Hartley, Chem. Soc. Rev. 2 (1973) 163–179.
[80] P. Surawatanawong, Y. Fan, M.B. Hall, J. Organomet. Chem. 693 (2008) 1552–1563.
[81] J.P. Stambuli, C.D. Incarvito, M. Buhl, J.F. Hartwig, J. Am. Chem. Soc. 126 (2004) 1184–1194.
[82] S. Moncho, G. Ujaque, A. Lledós, P. Espinet, Chem. Eur. J. 14 (2008) 8986–8994.
[83] F. Paul, J. Patt, J.F. Hartwig, Organometallics 14 (1995) 3030–3039.
[84] A.G. Sergeev, A. Zapf, A. Spannenberg, M. Beller, Organometallics 27 (2008) 297–300.
[85] J.-P. Corbet, G. Mignani, Chem. Rev. 106 (2006) 2651–2710.
[86] C. Sicre, A.A.C. Braga, F. Maseras, M.M. Cid, Tetrahedron 64 (2008) 7437–7443.
[87] G. Mann, Q. Shelby, A.H. Roy, J.F. Hartwig, Organometallics 22 (2003) 2775–2789.
[88] F. Barrios-Landeros, B.P. Carrow, J.F. Hartwig, J. Am. Chem. Soc. 130 (2008) 5842–5843.